THE ELECTROPLASTIC EFFECT IN TITANIUM

K. Okazaki*, M. Kagawa** and H. Conrad

Metallurgical Engineering and Materials Science Department
University of Kentucky
Lexington, Kentucky 40506, U. S. A.

Introduction

A number of investigations (1) have shown that a decrease in flow stress and an increase in the creep rate and stress relaxation occur upon going from the normal to the superconducting state, which indicates clearly a significant interaction between moving dislocations and electrons. Further, Troitskii (2) and co-workers have since 1969 proposed that the significant decrease in the flow stress which occurs when current pulses of the order of 10^3 A/mm^2 are applied for a duration of 10^{-4} s to the superconducting metals Zn, Cd, Sn, Pb and In undergoing uniaxial tensile deformation at a constant strain rate is due to an electron-dislocation interaction which they termed an electroplastic effect. Their results indicate that the amount of decrease in the flow stress per current pulse increases (up to 40%) with voltage and the number of carriers. It also increases with impurity content and decrease in temperature, but is reduced by an increase in strain rate.

Later, Spitsyn et al. (3) investigated the electroplastic effect in 18/9 stainless steel in tension and stress relaxation. They found that current pulses produced an increase in stress relaxation and a reduction of about 10% in the ultimate strength, indicating that the electroplastic effect is not limited to superconducting materials. The present authors (4) have confirmed that the electroplastic effect in fact occurs in all common crystal structures (fcc Pb, cph Ti, bcc Fe and tetragonal Sn), which were subjected to high current pulses during uniaxial tensile tests at room temperature. For a given current density, we found that the electroplastic effect increased in the order: Sn (tetragonal), Pb (fcc), Ti (cph) and Fe (bcc), suggesting that the electroplastic effect is related not only to the interaction of electrons with moving dislocations but also to the nature of the thermally activated overcoming of obstacles by dislocations inherent to the crystal structure. The present paper reports the results of a study into the electroplastic effect in titanium, giving attention to the effects of strain rate (0.67×10^{-4} to 16.7×10^{-4} s^{-1}), temperature (77 to 300 K) and interstitial solute content (0.2 to 1.0 at % oxygen equivalent) on the stress decrements associated with a single, high current pulse at both the flow stress level and at the internal stress level as a function of the current density.

Experimental

1.1 Materials and specimen preparation

The materials employed in the present study were: (a) a polycrystalline Ti (99.97%) wire of 0.5 mm diam. purchased from the Research Organic/Inorganic

---

*Presently with Allied Chemical Corporation, Morristown, New Jersey 07960, U. S. A.

**Graduate student, now with Hitachi Cable, Let., Tsuchiura, Ibaraki 317, Japan

Corp., U. S. A., (b) MARZ grade zone-refined Ti from the Materials Research Corp., U. S. A., (c) commercial A-50 Ti and (d) A-75 Ti. The total interstitial solute content of the polycrystalline Ti wire and MARZ Ti is estimated to be ~0.2 at%, that of A-50 Ti to be ~0.5 at% and that of A-75 Ti to be ~1.0 at%. The original as-swaged rods of 3.18 mm diam. for the latter three materials were rolled down at room temperature to 0.5 mm thick by 7.5 mm wide strips with an average reduction of cross-sectional area 20% per pass. At the intermediate thicknesses of 1.7 and 0.9 mm during rolling and after the final rolling samples were first mechanically polished to eliminate any macroscopic cracks and roll marks from the rolling and swaging operations. The intermediate thickness strips were chemically polished with a $HF\text{-}HNO_3$ solution and annealed for 1.8 ks at 1073 K in a vacuum of 10^{-3} Pa. The final thickness strips were sliced into 0.6 mm wide by 90 mm long specimens using a water-cooled diamond wheel cutter before the chemical polishing and vacuum annealing procedures.

1.2 Tensile tests

A conventional Instron universal testing machine (screw driven-hard beam type), whose crosshead speed can be varied from 0.01 to 4 mm/s and which has a maximum load capacity of 500 kg, was used. For the tensile tests at room temperature, a compressed air flow was used. A liquid nitrogen bath was used for tests at 77 K. Specially designed grips were used to clamp the specimen firmly and provide the desired electrical connection (Fig. 1). The specimen was firmly attached with a cyanoacrylate glue to 9.5 mm diam. steel balls through which holes had been drilled or which had been cut in half. The steel balls holding the specimen were placed into semi-spherical shape holes in stainless steel jigs, which were connected through universal joints and insulated coupling to the pull rod of the Instron machine. A screw type electric connector with a Pb-Sn solder-mounted contact was attached to a stainless steel jig to provide direct connection to the end of the specimen extending beyond the steel balls.

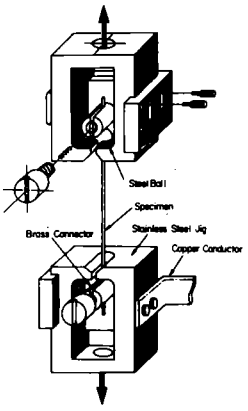

Fig. 1 Schematic of tensile fixture for electroplastic experiments

All the tensile tests were conducted with specimens of 50 mm gauge length. The partially unloaded states (long-range internal stress) were achieved by reversing the crosshead motion during a tensile test. To extract the contribution of the electron-dislocation interaction to the electroplastic effect, the stress decrements were measured in various deformation regions, namely (a) $\Delta\sigma_H$, in the initial elastic region of the stress-strain curve, (b) $\Delta\sigma_p$, in the plastic region of the stress strain curve, (c) unloading to an applied stress σ_a greater than the long-range internal stress σ_μ, (d) $\Delta\sigma_R$, at the stress level of $\sigma_a = \sigma_\mu$, and (e) at the stress level of $\sigma_a < \sigma_\mu$ (Fig.2). The details are given elsewhere (5).

1.3 Current pulsing apparatus

The present apparatus is designed to yield:

Voltage: 0 to 920 V
Current: 0 to 9000 A
Pulse Duration: 40 to 200 μs
Pulse rate: 0.1 to 20 pulses/s.

The schematic circuit diagram is shown in Fig. 3. The stored electrical energy in the capacitor bank can be discharged through a fast-response high capacity, vacuum ion switch specially designed for the present experiments. The characteristics associated with the present pulsing apparatus are given elsewhere (6).

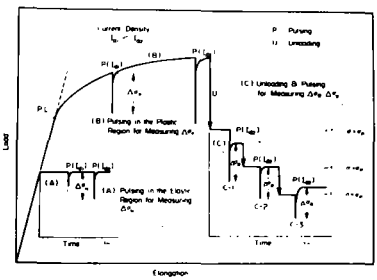

Fig. 2 Schematic of the $\Delta\sigma_H$, $\Delta\sigma_p$ and $\Delta\sigma_R$ measurements

Experimental Results

2.1 Specimen size effect

Klypin (7) and Troitskii and Stashenko (8) claimed that the electron flux or electric field might influence the properties of the metal surface, which could offer some assistance to dislocation motion by reducing the resistance to the egress of dislocations from the surface. If this is the case, the electroplastic effect should depend on the specimen size. Shown in Fig. 4 is the effect of current density on the decrease in stress due to current pulsing (4). A detailed study of the specimen size effect on $\Delta\sigma_p$, $\Delta\sigma_R$ and $\Delta\sigma_H$ (5) yielded a relatively constant slope when they are plotted versus the square of the specimen radius, indicating that the effect can be eliminated by extrapolating to $r^2=0$, and therefore the specimen size effect contained in $\Delta\sigma_p$ and $\Delta\sigma_R$ can be eliminated by subtracting $\Delta\sigma_H$ from them, namely

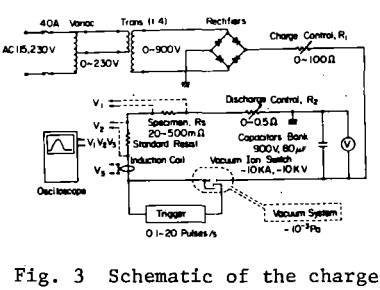

Fig. 3 Schematic of the charge-discharge circuit

$$\Delta\sigma_p^o = \Delta\sigma_p(r^2=0) = \Delta\sigma_p(r_1) - \Delta\sigma_H(r_1), \quad I_d = \text{const.} \qquad (1)$$

$$\Delta\sigma_R^o = \Delta\sigma_R(r^2=0) = \Delta\sigma_R(r_1) - \Delta\sigma_H(r_1), \quad I_d = \text{const.} \qquad (2)$$

so that $(\Delta\sigma_p - \Delta\sigma_H)$ and $(\Delta\sigma_R - \Delta\sigma_H)$ are independent of specimen diameter. This specimen size effect can then be considered in terms of a heating effect and a surface effect. The former becomes important when both the current density I_d is larger than 3000 A/mm^2 and the specimen diameter is larger than 0.3 mm while, the latter is important only when the diameter becomes less than 0.25 mm (the details are given in ref. 5).

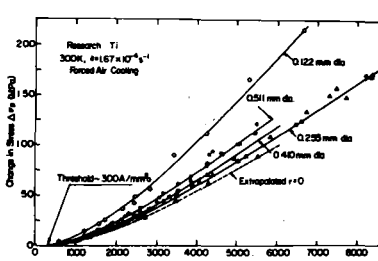

Fig. 4 Effect of current density on the decrease in stress due to pulsing as a function of the specimen diameter in Research Titanium

2.2 Skin and pinch effects (6)

Localization or concentration of current near a specimen surface (skin effect) is expected when a high frequency current is applied to a specimen. To establish whether or not the skin effect occurred in our experiments, the skin depth δ was calculated using the equation

$$\delta = (\pi f \mu (1/\rho))^{-1/2} \tag{3}$$

where f is the frequency of the pulse, μ the permeability and ρ the resistivity of the specimen. Typical values for the parameters in the above equation at 300 K are: f=9 kHz, μ=4 x10^{-7} H/m and ρ=8.2x10^{-6} Ωcm. Substituting these values into the equation gives δ=1.52 mm, which is about 6 times the radius of the largest size specimen (0.5 mm diameter), leading to the conclusion that the current is distributed uniformly throughout the specimen cross-section for our experimental conditions.

Upon the application of a high current pulse, a pinch effect may occur, whereby the pressure created by the intrinsic magnetic field produces radial compressive stresses. This pinch effect causes a decrease in the axial stress of a specimen undergoing tensile deformation at a constant plastic strain rate. In short, the decrease in axial stress due to this pinch pressure P will be

$$\Delta\sigma_{pinch} = 2\nu_p = 2\nu(1/4)\mu\, I_d^2(r^2 - a^2) \tag{4}$$

where ν is Poissons ratio, a the distance from the axis of the wire. Taking ν=0.34 gives the stress decrease, $\Delta\sigma_{pinch}$=0.33 MPa at 5000 A/mm^2. This is only 0.4% of the total change in the flow stress ($\Delta\sigma_p$=87.5 MPa at 5000 A/mm^2), 0.6% of $\Delta\sigma_R$(=55.0 MPa at 5000 A/mm^2) and 1% of $\Delta\sigma_H$(=32.5 MPa at 5000 A/mm^2) at 300 K. It is therefore concluded that the pinch effect associated with the current pulsing is small and only a secondary factor in the electroplastic effect in titanium.

2.3 Dependence of the electroplastic effect on strain rate, temperature and interstitial impurity concentration (9)

The changes in stress $\Delta\sigma_H$, $\Delta\sigma_p$ and $\Delta\sigma_R$ versus the current density are plotted as a function of the nominal strain rate during the tensile tests of the Ti wire at 300 and 77 K in Figs. 5 and 6, respectively. The three rates investigated at each temperature, namely 0.67x10^{-4}, 1.67x10^{-4} and 16.7x10^{-4} s^{-1} are indicated on the curve for $\Delta\sigma_p$. No significant effect of strain rate on $\Delta\sigma_p$ is evident. This was also the case for $\Delta\sigma_H$. Also $\Delta\sigma_R$ was not affected by the strain rate during the prior plastic deformation. Worthy of mention is that the curves of Figs. 5 and 6 were obtained only for increasing current density and strain; therefore they do not exhibit the loop shown in Fig. 2 of reference 5.

Comparing Figs. 5 and 6 we note two effects of decreasing the test temperature from 300 to 77 K; (a) the beginning of the curves is displaced slightly toward a higher current density and (b) the slopes of the curves become smaller. Upon substracting $\Delta\sigma_H$ from $\Delta\sigma_p$ and $\Delta\sigma_R$, it was found that the effects were due in large part to the better cooling efficiency of the liquid nitrogen bath at 77 K compared to the forced-air cooling at 300 K.

Depicted in Fig. 7 is the effect of current density on $\Delta\sigma_p$, $\Delta\sigma_R$ and $\Delta\sigma_H$ at 77 K as a function of interstitial impurity concentration in titanium. It is seen that all three stress-change parameters increase as the interstitial concentration increases. The increase in $\Delta\sigma_H$ with interstitial concentration is believed to be due to the resulting increased resistivity of the specimen, which leads to an increased heating effect.

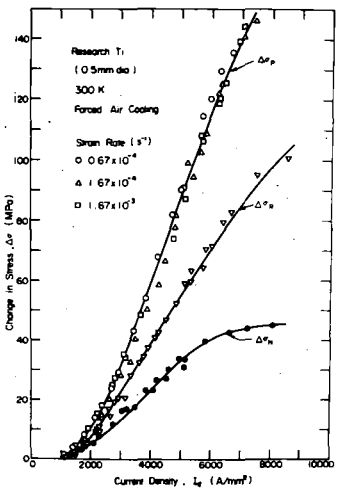

Fig. 5 Effect of current density on $\Delta\sigma_p$, $\Delta\sigma_R$ and $\Delta\sigma_H$ in Ti as a function of strain rate at 300 K

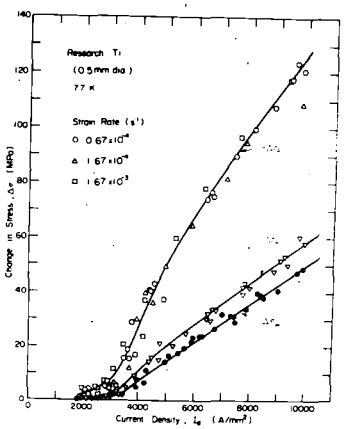

Fig. 6 Effect of current density on $\Delta\sigma_p$, $\Delta\sigma_R$ and $\Delta\sigma_H$ in Ti as a function of strain rate at 77 K

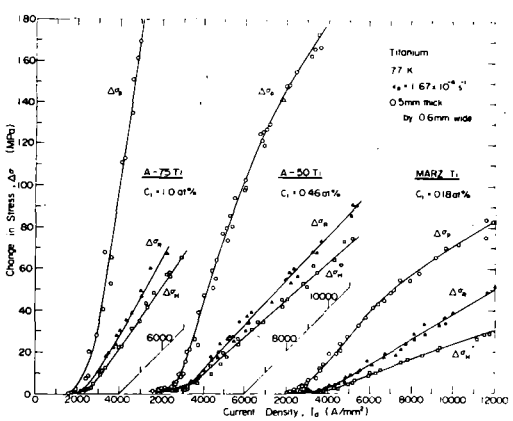

Fig. 7 Effect of current density on $\Delta\sigma_p$, $\Delta\sigma_R$ and $\Delta\sigma_H$, in Ti with various interstitial solute contents tested at 77 K

Let us take the stress change due to the effect of electrons on the mobile dislocations as

$$\Delta\sigma_e = \Delta\sigma_p - \Delta\sigma_R \tag{5}$$

whose physical significance has been discussed in detail elsewhere (9). The experimental results show that $\Delta\sigma_e$ increases significantly with the current density I_d but only slightly with temperature. The lack of a strain rate dependence in the range of 0.67×10^{-4} to 16.7×10^{-4} s^{-1} and no significant temperature dependence from 77 to 300 K are not in accord with the results previously reported by Troitskii et al (10, 11, 12). They found that the electroplastic effect in terms of $\Delta\sigma_p$ decreases with an increase in strain rate at higher rates and increases with increasing strain rate at lower rates. Also for the temperature dependence of $\Delta\sigma_p$, they found an increase in $\Delta\sigma_p$ with decreasing temperature. However, it should be noted that their strain rate and temperature dependences are on $\Delta\sigma_p$ which includes the influence of the heat generation and plastic straining and is not entirely due to the electron-dislocation interaction.

Generally most of the solution hardening phenomena can be expressed by

$$\Delta\sigma_e = \alpha' C_i^{n*} \tag{6}$$

where $\Delta\sigma_e$ is the change in stress due to solutioning and α' and n^* are constants. Analogously, the present results exhibit a linear relationship between $\Delta\sigma_e$ and C_i in log-log scale to yield

$$\Delta\sigma_e = \alpha C_i, \quad n^*=1.0 \tag{7}$$

where the constant α increases with I_d.

Discussion

Since detailed discussions have been given on the experimental results elsewhere (4, 5, 6, 9), the present discussion here is focused only on the effect of heating on the electroplastic effect and some interpretations of the measured parameters.

3.1 Effect of heating on the electroplastic effect

Let us calculate the influence on the electroplastic results of the actual temperature rise based on the current-time profile observed on an oscilloscope and heat transfer from the specimen surface. The temperature change $\Delta T(= T - T_o$, where T_o is the original temperature prior to pulsing a current) as function of time t during a current pulse is given by

$$\Delta T(t) = \Sigma\Delta Q'(t)/C_p M \tag{8}$$

where M and C_p are the mass and heat capacity of the specimen and $\Delta Q'(t)$ the net heat retained in the specimen at time t, which is taken to be

$$\Delta Q'(t) = (I^2(t)\ R(T) - HA(T - T_o))\Delta t \tag{9}$$

where I(t) is the current at time t, R(T) the resistance of the specimen at temperature T, H the heat transfer coefficient and Δt the time interval.

Assuming that the plastic strain change ε_p is due to thermally activated plastic deformation processes, we can write

$$\Delta\varepsilon_p = \dot{\varepsilon}_p\ \Delta t \tag{10}$$

where $\dot{\varepsilon}_p$ is the plastic strain rate which is included in the total strain rate

$$\dot{\varepsilon}_{total} = \dot{S}/\ell = \dot{\varepsilon}_p + \dot{\varepsilon}_e + \dot{\varepsilon}_H \tag{11}$$

where $\dot{S}$ is the crosshead speed, ℓ the gauge length, $\dot{\varepsilon}_e$ and $\dot{\varepsilon}_H$ are the elastic strain rate and the rate due to thermal expansion given by $\alpha(T)(T - T_o)$ with $\alpha(T)$ the linear thermal expansion coefficient at T. For titanium we have the choice of describing the rate equation for $\dot{\varepsilon}_p$ by either (13, 14)

$$\dot{\varepsilon}_p(1) = \beta(\sigma^*(T))^{m^*(T)} \tag{12}$$

where β is a constant, $\sigma^*(T)$ the effective stress (the applied stress minus long-range internal stress, σ_μ) and $m^*(T)$ its velocity exponent, or

$$\dot{\varepsilon}_p(2) = \dot{\varepsilon}_o \exp(-\Delta G(\sigma^*)/kT) \tag{13}$$

where $\dot{\varepsilon}_o$ is a constant and ΔG the Gibbs free energy given by

$$\Delta G = \Delta G_o(1 - (\sigma^*(T)/\hat{\sigma})^2) \tag{14}$$

where ΔG_o is the total energy at $\sigma^*(T)=0$. During a current pulse the effective stress $\sigma^*(T)$ is given by

$$\sigma^*(T) = \sigma_a - \sigma_\mu(T) - \Delta\sigma_a \tag{15}$$

where $\Delta\sigma_a$ is the change in flow stress which is equal to $-\Delta\varepsilon_e E_e$ (where E_e is the effective elastic modulus of the system).

A computor calculation was made using equations (8) to (15) for the change in the flow stress $\Delta\sigma_a$ during a current pulse under the conditions of:

Present Test Conditions	Parameters
$\sigma^*(T=300\ K) = 89.9$ MPa	$\sigma^*(T) = 6.43(515 - T)^{1/2}$ MPa
$\sigma_\mu(T=300\ K) = 65.0$ MPa	$\sigma_\mu(T) = 65.0 + 4.5\times10^{-2}(T - 300)$ MPa
$\hat{\sigma}_o^* = 294$ MPa	$\Delta G_o = 1.6$ eV
$E_e = 8.91\times10^4$ MPa	$m^*(T) = 1.94\times10^4/T^{1.29}$
$T_o = 300$ K	$C_p(T) = 0.51 + 4.22\times10^{-4}(T - 275)$ J/gK
$\varepsilon_o = 1.7\times10^{-4}\ s^{-1}$	$\alpha(T) = 2.04\times10^{-5}T^{1/4}$
$I_d = 4977\ A/mm^2$	$R(T) = (42 + 0.178(T - 300))\times2.54\times10^{-3}$ ohm
	$H = 2.9\times10^{-4}$ J/sKmm^2
	T in K

Typical results obtained using eq. (13) for the plastic strain rate are shown in Fig. 8, where the left side is drawn on a micro-second scale, whereas the right side on a second scale. To be noted in Fig. 8a is that the temperature rise ΔT increases with time, reaches a maximum of 137 K at $t=47\times10^{-6}$ s and remains at this level for a short period even after a pulse is gone. However, at longer time ΔT decreases with time and returns to the original temperature in about 4 s. Fig. 8a also shows that the maximum of $\Delta\sigma_a$ occurs at $t=47\times10^{-6}$ s; the maximum plastic strain ε_p produced by thermal activation at this time is of the order of only 10^{-8}. This implies that the expected stress change $\Delta\sigma_{\Delta T}$ from thermal activation processes is only of the order of 10^{-4} MPa and therefore the total stress change $\Delta\sigma_a$ is almost entirely due to the thermal expansion, which reduces the effective stress σ^* to a negative value. In other words, the thermal expansion brings the stress level down so quickly and so low that insufficient effective stress is available to produce a significant amount of plastic strain. However, once the temperature begins to decrease (Fig. 8b), σ^* increases to produce the plastic strain (strain rate) which is required by the crosshead motion. It reaches its original value after about

1.4 s, when the plastic strain rate imposed by the crosshead motion first approaches that prior to the current pulse. The results of Fig. 8 thus indicate that by assuming no contribution of the current to σ^*, thermally activated deformation cannot provide significant plastic strain within the time period (0.3 s) of the measured stress $\Delta\sigma_p$, and therefore indicate that the heating produced by a current pulse causes a thermal expansion of the specimen but does not lead to any significant plastic flow.

To account for the required plastic strain and to simulate the stress change $\Delta\sigma_p$ observed in the experiments, an electron-dislocation interaction is now assumed to occur and is taken to be of the form

$$\Delta\sigma_{ep} = \beta_e I_d \tag{16}$$

where I_d is the current density and β_e a constant. This proportionality between $\Delta\sigma_{ep}$ and I_d is presently assumed because theory (15, 16) and the previous results on the electroplastic effect in titanium (4, 5, 6) suggest a linear relationship between them. Thus, $\Delta\sigma_{ep}$ is added to $\sigma^*(T)$ giving

$$\sigma^*_{total} = \sigma^*(T) + \Delta\sigma_{ep} \tag{17}$$

and inserted in eq. (14) to yield

$$\Delta G = \Delta G_o \left(1 - ((\sigma^*(T) + \Delta\sigma_{ep})/\sigma^*_o)^2\right). \tag{18}$$

A computation is then made under the same conditions as those of Fig. 8. The results are presented in Fig. 9, where $\beta_e = 0.019$ (in $\Delta\sigma_{ep}=\beta_e I_d$) has been used to produce the plastic strain of 4.2×10^{-4}, which is equivalent to $\Delta\sigma_{ep}$=34.5 MPa. It is seen in Fig. 9 that $\sigma^*(T)$ is now reduced rather more quickly and steeply than in Fig. 8 and that $(\sigma^*(T) + \Delta\sigma_{ep})$ exhibits a peak of 126 MPa at 8×10^{-6} s, giving a maximum plastic strain rate of 4.8×10^{1} s^{-1}. With this contribution of $\Delta\sigma_{ep}$ to σ^* a significant amount of plastic strain (four orders of magnitude larger compared to the case without $\Delta\sigma_{ep}$ shown in Fig. 8) is now produced before 20×10^{-6} s. It should be also noted that the temperature rise does not now entirely determine the production of the plastic strain during the microsecond time scale. Again, once the pulse is gone, the temperature begins to decrease (Fig. 9b) and ε_p starts to increase again after 2.7 s, at which time the effective stress σ^* becomes equal to that for plastic flow at the strain

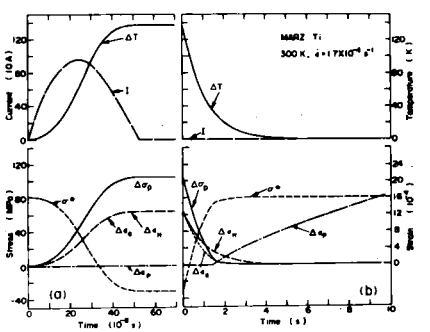

Fig. 8 Computor simulation of ΔT, σ^*, $\Delta\sigma_p$, $\Delta\varepsilon_e$, $\Delta\varepsilon_H$ and $\Delta\varepsilon_p$ at 300 K for the current pulse I shown, assuming no effect of current on σ^*.

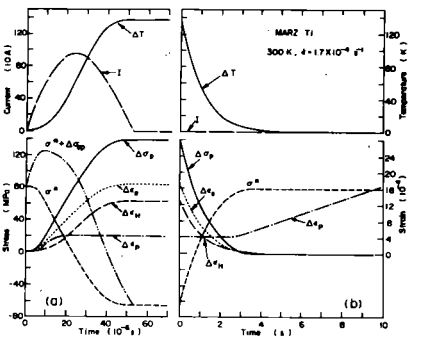

Fig. 9 Computor simulation of ΔT, σ^*, $(\sigma^* + \Delta\sigma_{ep})$, $\Delta\sigma_p$, $\Delta\varepsilon_e$ and $\Delta\varepsilon_H$ at 300 K for the current pulse I shown, assuming a contribution of $\Delta\sigma_{ep} = 0.019\ I_d$ to σ^*.

rate imposed by the crosshead motion. It is worthy to note that $\Delta\sigma_{ep}$ at the maximum of $(\sigma^* + \Delta\sigma_{ep})$ is about ~0.8 σ^*; further, $\Delta\sigma_a$ at 0.3 s in Fig. 9 is 32 MPa larger than in Fig. 8 for the same time. From these computor calculations, we come to the conclusion that the current pulse provides an extra stress $\Delta\sigma_{ep}$ in addition to any heating effects. Taking the measured value of $\Delta\sigma_p$ equal to $\Delta\sigma_a$ at 0.3 s in Fig. 9 the electroplastic contribution from Figs. 8 and 9 come to 32% of $\Delta\sigma_p$.

3.2 Physical interpretation of the measure parameters

In the previous computor simulation of the electroplastic effect, we had two unknown parameters to be assumed; the heat transfer coefficient H and an additional effective stress $\Delta\sigma_{ep}(t)$ due to pulsing. Experimentally we could observe $\Delta\sigma_{ep}$ only on the second-scale when a pulse was applied at the flow level, while $\Delta\sigma_{ep}$ should not exist at the long-range internal stress level. Therefore, it is possible to evaluate H using a curve fitting technique to the observed stress change $\Delta\sigma_R(t)$ as a function of time t. Taking MARZ Ti forced-air colled at 300 K with I_d=3143 A/mm^2, a minimum deviation was achieved by a value of H=6.32x10^{-4} Js^{-1}mm^{-2}. Once H was determined, the experimental data for $\Delta\sigma_p(t)$ was used to curve-fit to find $\Delta\varepsilon_{ep}$ through a relation of $\Delta\sigma_p=E_e\Delta\varepsilon_{ep}$. For example, the obtained $\Delta\varepsilon_{ep}$ for Research Ti at 300 K with I_d=3162 A/mm^2 could be converted into the stress via E_e to yield $\Delta\sigma_e^*$=8.5 MPa. On the other hand, the measured value of $\Delta\sigma_e(=\Delta\sigma_p - \Delta\sigma_R)$ under the same condition was 6.0 MPa. The measured value of $\Delta\sigma_e$ is approximately 30% less than $\Delta\sigma_e^*(=\Delta\sigma_p^{max}(t) - \Delta\sigma_R^{max}(t))$ obtained from computor simulation. This difference stems from the slow response of the stress monitoring system (1.0 s/full scale) presently employed, which is approximately equivalent to the actual error in $\Delta\sigma_e$ measured (about 20% less than $\Delta\sigma_e$ measured with a faster recording system of 0.5 s/full scale).

The computor simulation clearly shows the physical meaning of the measured parameters $\Delta\sigma_R$ and $\Delta\sigma_p$ to be: (a) $\Delta\sigma_R$ is only due to the thermal expansion via the generated Joule heat, (b) $\Delta\sigma_p$ is due to the same thermal expansion as $\Delta\sigma_R$

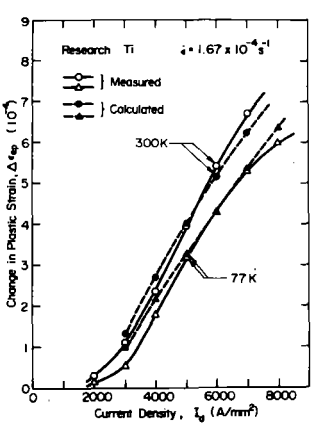

Fig. 10 Comparison between computor-generated and experimentally-measured I_d-$\Delta\sigma_{ep}$ relationships in Ti at 77 and 300 K.

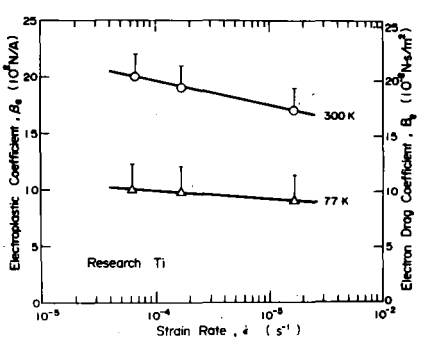

Fig. 11 Calculated electroplastic and electron drag coefficients versus strain rate as a function of temperature.

plus the resultant plastic strain increment $\Delta\varepsilon_{ep}$ from a current pulse, and (c) the experimentally measured $\Delta\sigma_p$ and $\Delta\sigma_R$ are influenced by the damping effect of the linear recorder employed. However, the difference between $\Delta\sigma_p$ and $\Delta\sigma_R$, ie. $\Delta\sigma_e$, only differs -15 to -20% from the computor difference $\Delta\sigma'_e(=B_e\Delta\varepsilon_{ep})$. Taking into consideration other possible experimental errors of ±10%, the measured $\Delta\sigma_e(=\Delta\sigma_p - \Delta\sigma_R)$ includes an error of -5 to -30%.

Depicted in Fig. 10 is the calculated $\Delta\varepsilon_{ep}$ versus current density I_d for Research Ti at 77 and 300K, along with the experimentally observed $\Delta\sigma_{ep}$. Considering possible errors in the physical parameters used for the simulation, the computor simulated $\Delta\varepsilon_{ep}$-I_d relationship agrees with the experimentally measured relationship at both temperatures. This agreement supports the validity of the assumption given by eq. (16), which leads to the conclusion that the interaction between the electron flux and moving dislocation is of a friction type.

The values of β_e obtained by the present simulation using the experimentally measured values of $\Delta\varepsilon_{ep}$ for a pulse of I_d=5000 A/mm^2 are plotted against the strain rate as a function of temperature in Fig. 11. Only a slight increase in β_e with a decrease in strain rate is observed, whereas the values of β_e at 300 K are approximately twice those at 77 K. Because of the small value of the average dislocation velocity, $\bar{v}$ (~10^{-3} cm/s) compared with the electron drift velocity $\bar{v}_e$ (13.8cm/s at I_d=5000 A/mm^2) the contribution of $\bar{v}$ to the relative velocity between drifting electrons and moving dislocations can be neglected. Then we can define

$$\Delta\sigma_{ep} = B_e \bar{v}_e/b = \beta_e I_d \qquad (19)$$

where b is the Burgers vector, and the calculated values of B_e (0.19×10^{-6} Ns/m^2 at 300 K and 0.10×10^{-6} Ns/m^2 at 77 K) are within the range of theoretically calculated values (10^{-3} to 10^{-8} Ns/m^2) by Mason (17), Holsterin (18), Kravchenko (15) Huffman et al (19) and Brailsford (20) for the electron drag effect. Further detailed discussion on the nature of the interaction will be given elsewhere.

References

1. For example, G. Kostorz, phs. stat. sol., (b) 58 (1973), 9
2. For example, O. A. Troitskii, Probemy Prochnosti, 7 (1975), 14
3. V. I. Spitsyn, O. A. Troitskii, E. V. Gusov and V. K. Kurdynkov, Invest. Akad. Nauk, SSSR, Metallg., No. 2 (1974), 124
4. K. Okazaki, M. Kagawa and H. Conrad, Scripta Met., 12 (1978), 1063
5. K. Okazaki, M. Kagawa and H. Conrad, Scripta Met., 13 (1979), 277
6. K. Okazaki, M. Kagawa and H. Conrad, to be publ. Mater. Sci. and Eng.
7. A. A. Klypin, Problemy Prochnosti, No. 7 (1975), 20
8. O. A. Troitskii and V. I. Stashenko, Fiz. Metl. Metallov. 47 (1979), 180
9. K. Okazaki, M. Kagawa and H. Conrad, Scripta Met., 13 (1979), 473
10. O. A. Troitskii and A. G. Rozno, Fiz. Metal. Metalov, 30 (1970), 824
11. V. I. Spitsyn and O. A. Troitskii, Dokl. Akad, Nauk SSSR, 216 (1974), 1266
12. O. A. Troitskii, Fiz. Metal. Metallov., 32 (1971), 408
13. K. Okazaki and H. Conrad, Trans JIM, 13 (1972), 205
14. K. Okazaki, T. Odawara and H. Conrad, Scripta Met., 11 (1977), 205
15. V. Ya. Kravchenko, Zh. Eksp. Tear. Fis., 51 (1966), 1676
16. K. M. Klimov, G. D., Shaynev and I. I. Novikov, Dokl. Akad. Nauk, SSSR, 219 (1974), 323
17. W. P. Mason, Phys. Rev., 143 (1966), 229, J. Accoust. 32 (1960), 458
18. T. Holstein, in App. of B.R. Tittman and H.E. Bommel, Phys.Rev.151 (1966) 178
19. G. P. Huffman and N. P. Louat, Phys. Rev. 176 (1968), 773
20. A. D. Brailsford, Phys. Rev., 186 (1969), 959